

MAGNETIC AND STRUCTURAL PROPERTIES OF γ -Fe₂O₃ NANOPARTICLES DISPERSED IN A SILICA MATRIX

I. Hrianca, C. Caizer, C. Savii^a, M. Popovici^a

West University of Timisoara, Faculty of Physics, Department of Electricity and Magnetism, Bd. V. Parvan no.4, 1900-Timisoara, Romania

^aRomanian Academy, Timisoara Branch, Inorganic Chemistry Laboratory, Bd. M. Viteazu no.4, 1900 Timisoara, Romania

Using ferric chloride and tetraethylorthosilicate (TEOS) as precursors, acetic acid and isopropyl alcohol as additives, and ethyl alcohol as solvent, Fe₂O₃:SiO₂ (30÷70 %; 70÷30 % molar ratio)- EtOH:TEOS:H₂O (17.5:1:16 molar ratio) xerogels were prepared. Fe₂O₃ nanoparticles formation in amorphous SiO₂ by xerogel annealing at 100 °C, 200 °C, 900 °C and 1100 °C is presented. The samples were examined by X-ray diffraction (XRD), infrared spectrometry (IRS) and dc magnetic measurements. Ferrimagnetic phase occurs after 900 °C heating; superparamagnetic behavior was observed after 200 °C heating and amorphous antiferromagnetic Fe₂O₃ phase was found after 100 °C heating. The increase of Fe ions leads to larger particle dimensions and the annealing temperature is decisive in different Fe₂O₃ phases formation.

Keywords: Ferric oxide, Sol-gel, Nanoparticles, XRD, IRS, Static curves of magnetization

1. Introduction

In the last years, the interest of the study concerning nanoparticle systems was improved, in the first place, because of the peculiarities observed in their magnetically behaviour, comparing the same bulk materials [1-5]. The nanoparticle's dimensions and shape together with magnetostatic interactions among them, have an important influence upon macroscopic magnetic properties (magnetisation, coercive field, magnetic susceptibility) of the system [6-8]. Particles γ -Fe₂O₄ are known being utilised successful as magnetic recording media [9-12]. Particle size reduction toward the monodomain configuration allows both an arising density in this media and the appearance of interesting, magnetic properties. Mutual particle magnetostatic interactions are significantly limited or even eliminated by their dispersion over a (crystalline), amorphous, nonmagnetic solid matrix [13-14]. On the other hand the grate interest for these systems is due to the possibility to obtain a reduced switch time of the saturation magnetisation (nanoseconds). To obtain the dispersed magnetic nanoparticles in amorphous silica matrix the sol-gel processing was used, which permits rigorous control of a narrow particle size distribution [15]. In this paper, we presents investigations concerning some structural and magnetic properties of the Fe₂O₃ (γ -Fe₂O₃ and α -Fe₂O₃) nanoparticles in SiO₂ matrix, obtained starting from tetraethylorthosilicate (TEOS) and ferric chloride hexahydrate FeCl₃.6H₂O precursors.

2. Experimental

A series of iron oxide silica composites were prepared by mixing an alcoholic solution of TEOS (Fluke) and aqueous solution of iron chloride (FeCl₃.6H₂O, Fluka A.G. puriss, p.a.), using a small amount of acetic acid (CH₃COOH) in water and ethyl alcohol (C₂H₅OH) as mutual solvent

following a procedure described elsewhere[gr]. Sol-gel process was carried out under high acidic conditions, at pH<2, in order to prevent the precipitation of the iron hydroxides. The Fe₂O₃:SiO₂ ratio was (70 : 30)%, samples A, respectively (30 : 70)%, samples B. After gelation at room temperature, in covered weasels, the obtained xerogels were slowly dried at 100 °C, at constant weight (samples A1, respectively B1). The dried xerogels were fired, at 200 °C (sample A2, respectively B2), 900 °C (sample A3) and 1100 °C (sample B3) and kept 60 minutes at each temperature.

The structural evolution of the samples, during thermal treatment, was monitored by thermal analysis (Paulik-Paulik-Erdey Derivatogrph), IR spectroscopy (SPECORD M 80 spectrometer) and X-ray diffraction (XRD). The XRD spectra was carried out using a DRON II Diffractometer with Cu K α wavelength (1,54056 \AA).

Magnetic measurements were performed on a standard equipment, based on the fluxmetric method connected to a data acquisition computing system (PC). The cylindrical shape of the measured sample was characterised by the following dimensions, 45 mm high and 4.5 mm in diameter. The utilised software permits to introducing of the demagnetisation field correction.

3. Results and discussions

Each temperature treated sample has been structural and magnetically characterised. X-ray diffraction patterns, Fig. 1 and Fig. 2, shows the amorphous state of the samples A1 and B1 (dried xerogels). In the case of 200 °C fired sample, A2, the appearance of the small picks attributed to γ -Fe₂O₃ crystalline phase it's obvious.

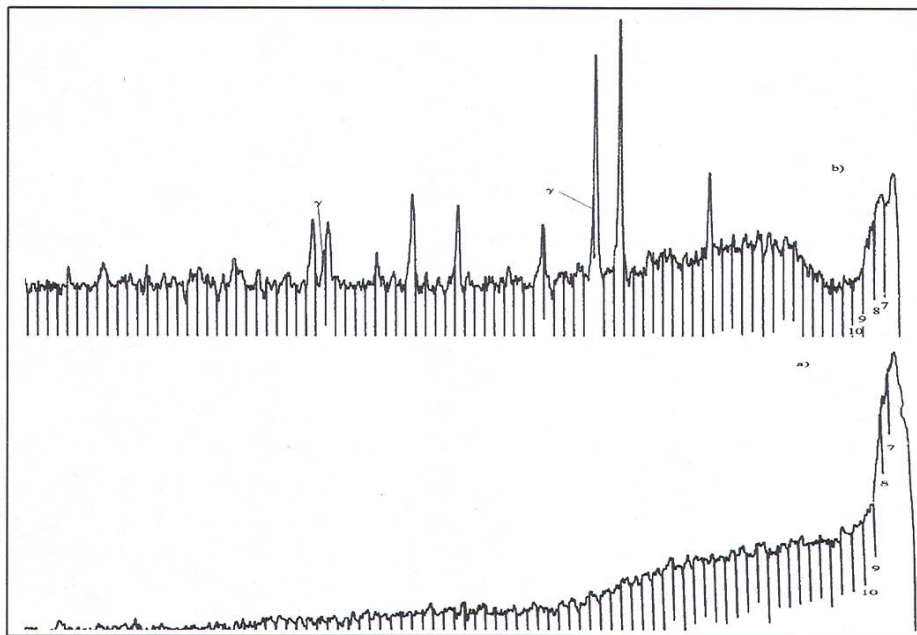


Fig. 1. XRD spectra for the sample A1 (a) and A3 (b).

After 900 °C (sample A3) respectively 1110 °C (sample B3), annealed iron oxide-silica composite, the XRD spectra put in evidence the diminishing intensity of the γ -Fe₂O₃ phase, with increasing temperature (200-900) °C and the appearance of the stable and well crystallised phase. At 900 °C γ -Fe₂O₃ phase concentration is under 10 % comparing approximately 90 % α -Fe₂O₃. At 1100 °C, γ -Fe₂O₃ phase concentration was unobservable on XRD spectra. According to literature [16] among other factors, utilising ferric chloride in stead of ferric nitrate as reactant favours α -Fe₂O₃ phase formation.

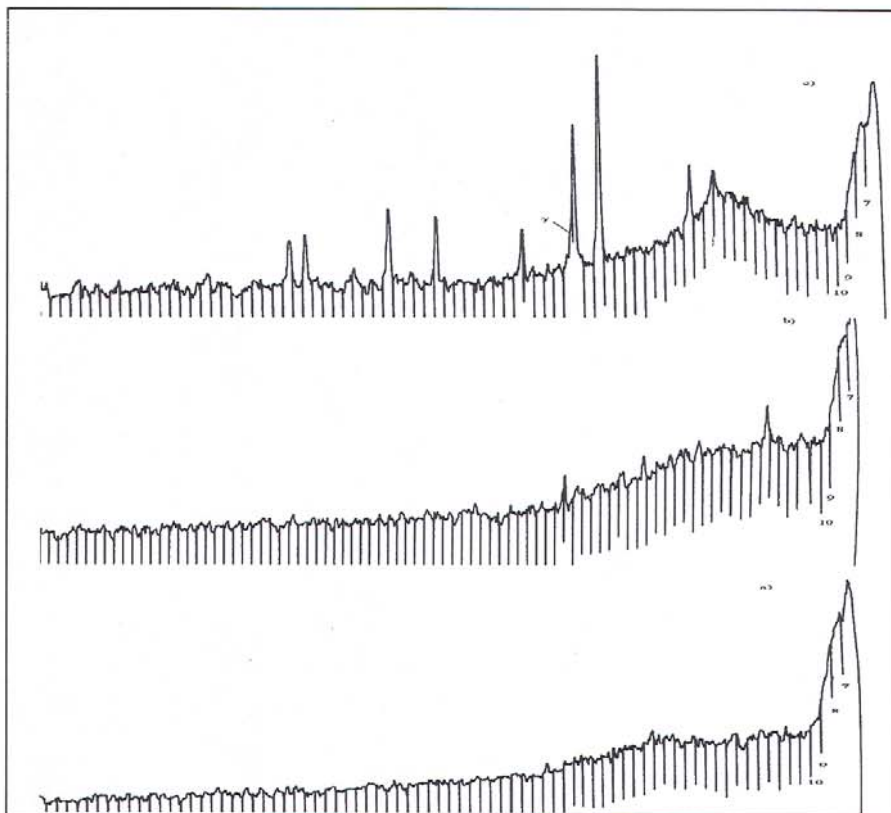


Fig. 2. XRD spectra for the sample B1 (a), B2 (b) and B3 (c).

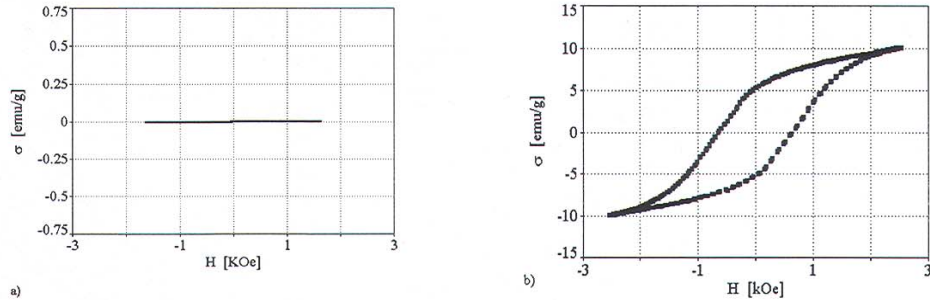
Particle size average, determined from XRD spectra, utilising Scherrer equation [17]

$$D(311) = 0.9 \lambda / \beta_{1/2} \cos \theta \quad (1)$$

where, $\beta_{1/2}$ is the full width at half maximum corresponding to (311) crystalline plan, θ is the Bragg angle and λ is the X-ray wavelength. Particle size average dimension is dependent on synthesis conditions and it increases with arising temperature during thermal treatment, the smallest particle size being observed at 200°C (~7 nm) [18].

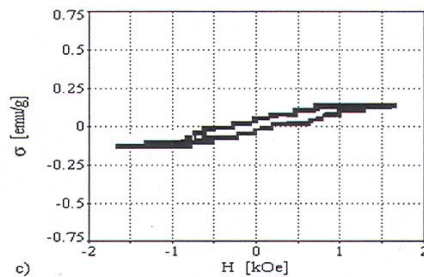
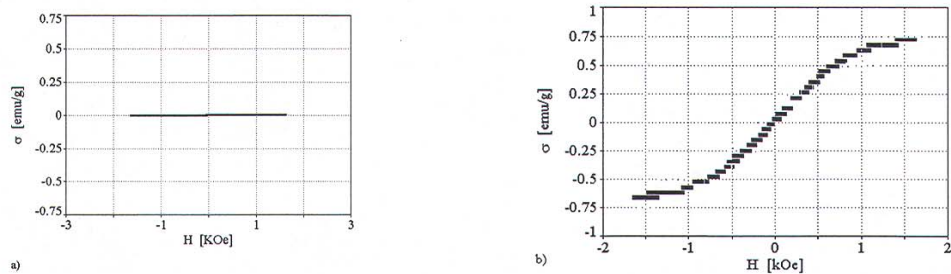
IR spectra recorded in the 4000-200 cm^{-1} range, coupled with thermal analysis data show the thermal evolution of the composition and structure of the xerogels. Increasing temperature leads to diminishing and disappearance of specific vibration peaks due to adsorbed water, Si-OH or organic radicals bonds confirmed by TG and ATD curves. In the same time it can be observed the Si-O-Si, (800, 1080 cm^{-1}), Fe-O (650-330 cm^{-1}) specific vibrations development [18].

Magnetic measurements put in evidence a different behaviour of the nanoparticles system at different temperatures and iron oxide concentrations in silica matrix, as it shown in the Fig. 3 and Fig. 4. The magnetisation curve shows an antiferromagnetic behaviour [19] of the both A1 and B1 xerogels (dried at 100°) corresponding to amorphous Fe_2O_3 present in the system (Fig. 3a and Fig. 4a). The reduced saturation magnetisation values of the samples B3, $\sigma_s = 0.13 \text{ emu/g}$ (Fig. 4c) comparing those of the bulk material $\gamma\text{-Fe}_2\text{O}_3$, $\sigma_s = 76 \text{ emu/g}$ [20] prove the antiferromagnetic $\alpha\text{-Fe}_2\text{O}_3$ was the predominant crystalline phase, confirmed by the XRD investigations (Fig. 2c). This result can be attributed to the higher temperature of the thermal treatment (1100 °C) which favourites $\alpha\text{-Fe}_2\text{O}_3$ more stable phase [16]. The magnetic hysteresis loop presence at this temperature could be considered as a consequence of both, the increased Fe_2O_3 concentration (30%) and the elevated



(A)

Fig. 3. Magnetisation curve, sample A1 (a), and magnetic hysteresis loop, sample A2 (b).



(B)

Fig. 4. Magnetisation curve, sample B1 (a) and magnetic hysteresis loops, sample B2 (b) and B3 (c).

temperature of thermal treatment. All these factors are leading to the rising ferrimagnetic γ -Fe₂O₃ particle size [15] and agglomerated particles. The mentioned effect is more obvious for the sample A3 (Fig. 3b), because of the concentration of iron oxide (70%) in silica matrix being 2.33 times greater. It can be expected, in this case, the nanoparticle system magnetic behaviour to be comparable to the bulk material. However, the saturation magnetisation value registered for A3 sample was $\sigma_s = 10$ emu/g, represents about a half from those reported in literature ($\sigma \sim 20$ emu/g) for γ -Fe₂O₃ nanoparticle system [20]. The found diminished value can be attributed both to the α -Fe₂O₃ presence in the system and to the magnetostatic interactions among the particles. It can not be excluded the possibility of the multidomianal nanoparticle in the mentioned system, which can be magnetised by Bloch walls displacements supplementary mechanism. In the case of reduced concentrations and temperatures, the nanoparticle system had a superparamagnetic behaviour (Fig. 4b). In this case saturated magnetisation $\sigma_s = 0.71$ emu/g, greater than those corresponding to the temperature 1100 °C ($\sigma_s = 0.13$ emu/g). The increased magnetisation can be attributed to the ferrimagnetic γ -Fe₂O₃ phase, predominant presence in the system, because of it's thermodynamic stability in such conditions.

Particle dimensions being reduced at 200 °C, it is possible to be monodimensional, and their magnetic moments can suffer fluctuations along the easy magnetisation axis (180° rotation) due to the thermal movement. Following the Neel theory, the relaxation time τ , results from the expression:

$$\tau = \tau_0 \exp (KV / kT), \quad (2)$$

where, $\tau_0 = 10^{-9}$ s, K represents the uniaxial anisotropy constant of the spherical particle, V is the particle volume, k Boltzmann constant and T temperature. Assuming $D(311) = 7$ nm, and $K = 1.8 \times 10^4$ J/m³ [21], it was obtained $\tau = 2.18$ ns. As long this value is much smaller than the required measurement time, $t = 20$ ms, the magnetic moments follow the applied magnetic field variations and the system behaviour is superparamagnetic.

4. Conclusions

Using a sol-gel processing, a nanoscale particle size, in the Fe₂O₃-SiO₂ system, has been obtained. TEOS and FeCl₃ precursors, in the described conditions of the process, have lead to the antiferromagnetic α -Fe₂O₃ as predominant crystalline phase formation and a small amount of γ -Fe₂O₃. At elevated temperatures (900 – 1100 °C) the stable α -Fe₂O₃ phase development is favoured. Both, the molar ratio Fe₂O₃: SiO₂ and thermal treatment temperature have a significant influence upon the particle size. Thus, at the 200°C and (30:70) Fe₂O₃: SiO₂ molar ratio, the γ -Fe₂O₃ nanoparticles had lower dimension and they are magnetic isolated in silica matrix, the reason because the system had a superparamagnetic behaviour. Contrary, taking into consideration higher Fe₂O₃ concentration (70%) in silica matrix and higher temperature (900 °C), the system was characterised by ferrimagnetic behaviour as a consequence of the concentration and nanoparticles average dimension increasing. This is leading to the frequent particles agglomerations occurrence, because of magnetostatic interactions among them. At 100 °C (dried xerogels) the antiferromagnetic amorphous phase Fe₂O₃ is dominant.

References

- [1] A. Chatterjee, D. Das, S. Prodhon, D. Chakravorty, *J. Magn. Magn. Mater.*, **127**, 214 (1993).
- [2] E. Brunshman et al., *J. Appl. Phys.*, **75**, 5882 (1994).
- [3] I. Hrianca, I. Malaescu, *J. Magn. Magn. Mater.*, **150**, 131 (1995).
- [4] C. Wang et al., *Mater. Research Bull.*, **33**, 1747 (1998).
- [5] I. Hrianca, I. Malaescu, C. Caizer, N. Stefu, S. Novaconi, *Rom. J. Phys.*, (1999) (accepted to published).
- [6] D. L. Leslie-Pelechy et al., *IEEE Trans. Magn.*, **34**, 1018 (1998).
- [7] G. Li, A. Chiba, S. Takahashi, M. Sato, *J. Appl. Phys.*, **83**, 3871 (1997).
- [8] T. Atarashi, Y. S. Kim, T. Fujita, K. Nakatsuka, *J. Magn. Magn. Mater.*, **201**, 7 (1999).
- [9] C. Bate, J. K. Alstad, *IEEE Trans. Magn.*, **5**, 821 (1969).
- [10] A. A. Giessen, *Rev. Phys. Appl.*, **9**, 869 (1974).
- [11] A. R. Corradi, *J. Magn. Magn. Mater.*, **7**, 233 (1978).
- [12] E. A. Dragisma et al., *J. Magn. Magn. Mater.*, **193**, 384 (1999).
- [13] D. Niznansky, J. L. Rehspringer, M. Drillon., *IEEE Trans. Magn.*, **30**, 821 (1994).
- [14] F. Bentivegna et al, *J. Appl. Phys.*, **83**, 7776 (1998).
- [15] C. Cannas et al. *J. Phys. Chem.*, **B 102**, 7721 (1998).
- [16] F del Monte et al., *Langmuir*, **13**, 3627 (1997).
- [17] H. P. Klug, L. E. Alexander, *X-Ray Diffraction Procedure*, 2-nd Edition, Wiley and Sons, Inc., New-York, 1974.
- [18] C. Savii, P. Miha, M. Enache, I. Hrianca, A. Zanfir, R. Turicin, C. Caizer, *Proc. 2 nd Intern. Conf. Chem. Sci. Sust. Develop.*, June 6-9, 2000, Halkidiki, Grecia.
- [19] C. Cannas et al., *Z. Naturforsch.*, **54a**, 513 (1999).
- [20] L. Zhang, G. C. Papaefthymiou, J. Y. Yng, *J. Appl. Phys.*, **81**, 6892 (1997).
- [21] P. V. Hendriksen, F. Boldker, S. Wells, S. Morup, *J. Phys.: Condens. Matter.*, **6**, 3081 (1994).